Chapter 2
Solar Oscillations

As a considerable number of reviews have been written on the subject of solar oscillations, and as this thesis is mainly concerned with the various stages of the reduction of observational data, I will not go into detail on the various theoretical aspects of solar oscillations. In particular, *Solar Interior and Atmosphere* (1991) edited by Cox, Livingston and Matthews, contains reviews of many areas of helioseismology and solar physics in general. As many of the chapters were written up to two years ago, they are not totally up to date, but the book does present a nice overview.

For general reviews of the theoretical properties of the solar oscillations, see for instance, Christensen-Dalsgaard and Berthomieu (1991) in *Solar Interior and Atmosphere.*

Some of the observational aspects have been reviewed by Hill, Deubner and Isaak in *Solar Interior and Atmosphere.*

In this chapter I will start with a brief historical introduction, followed by short discussion of some of the physical properties of the oscillations, especially those relevant for the subjects discussed in the rest of the thesis.

2.1 The Discovery of Solar Oscillations

While the field of helioseismology still has a certain flavor of being a 'new' field, the original observations that led to the discovery of the field are more than 30 years old.

The first observation of a periodic Doppler velocity signal on the Sun was reported in Leighton, Noyes, and Simon (1962) (see also Leighton 1959; Noyes and Leighton 1963) and soon thereafter in Evans and Michard (1962), but the correct physical cause of the oscillations was not immediately recognized.

In the years after the discovery, several different mechanisms for the observed oscillations were proposed, generally based on various atmospheric phenomena. The true cause of the phenomenon (that it is due to trapped acoustic waves in the solar interior) was first reported by Ulrich (1970) and Leibacher and Stein (1971).

The first 'hard' observational evidence for this theory was, despite considerable effort, not reported until several years later, when Deubner (1975) showed that the power in the oscillations was indeed concentrated along ridges in a so-called $k-\omega$ diagram (discussed later in this chapter), as predicted by the theory.

Even then, the fact that the modes represented truly *global* oscillations was not established. The first observations demonstrating that at least some modes were sufficiently long lived to be considered global, were probably those reported by Claverie et al. (1979), which showed that low-l modes observed in Doppler shift of integrated sunlight were separated in frequency with the expected spacing. Similar observations from the South Pole (which allows for longer uninterrupted time-series), were reported by Grec, Fossat, and Pomerantz (1980).

After this several observational programs were undertaken and soon modes with a large range of ls and frequencies were observed. Among the developments since then were the use of the oscillations to trace the velocity fields (the rotation) by Deubner, Ulrich, and Rhodes (1979) (see however, Rhodes, Harvey, and Duvall 1983), observations of frequency splittings of the deeply penetrating modes by Claverie et al. (1981), indicating a rapidly rotating solar core, and Duvall and Harvey (1983, 1984), who reported the first results of global (although one-dimensional) observations. These results were also the input to the first inversions for the radial dependence of the solar rotation rate (Duvall, et al. 1984).

The first observations of two-dimensional Doppler velocity images of the whole visible part of the Sun were those of Brown (1985). These observations were the first capable of resolving both the radial and the latitudinal variation of the solar rotation rate over a substantial fraction of the solar interior. Incidentally, the observations used in this thesis are a continuation of this program.

According to Brown (personal communications), the first group to do things 'right' was the BBSO group led by Libbrecht (see eg., Libbrecht 1988). Also, the South Pole group (see eg., Jefferies et al. 1988) has contributed significantly in the area of spatially resolved observations.

In the future very high quality full disk data is expected from the GONG network, which should start operations in 1994 and the SOI/MDI experiment on the SOHO satellite, due to be launched in 1995.

2.2 Basic Theory of Oscillations

As already mentioned, several excellent reviews of the general physical properties of solar oscillations exist (Christensen-Dalsgaard and Berthomieu 1991; Gough and Toomre 1991), and only a rudimentary overview will be given here.

As the amplitudes of the solar oscillations are very low, they are generally well represented by linear theory, in which the oscillations are viewed as a small perturbation on a (time-independent) background equilibrium state. For the present purpose, it is also assumed that the oscillations are adiabatic, that is, the motion is conservative. This is generally a very good approximation over the bulk of the solar interior, but close to the surface it breaks down, which will be discussed briefly later. The neglect of the nonadiabaticity does lead to minor errors in the mode frequencies and other properties. These two assumptions simplify the calculations of mode frequencies and eigenfunctions very considerably, and as a matter of fact, it is has proved very difficult to treat these two effects properly.

Also in the first approximation, the Sun may be treated as spherically symmetric (see the next section for a major problem with this). This assumption, combined with the assumption of a time-independent background state, means that the spatial variation of a mode, if written in spherical coordinates (r, θ, ϕ), where θ is colatitude and ϕ longitude, can be separated into a dependence on radius r and the angular coordinates θ and ϕ, described by spherical harmonics

$$Y_l^m(\theta, \phi) = P_l^m(\cos\theta)e^{im\phi}. \tag{2.1}$$

Here l is the degree and m the azimuthal order of the spherical harmonic Y_l^m, and P_l^m an associated Legendre function, which here has been normalized to have unit integral

$$\int_{-1}^{1} P_l^m(x)^2 dx = 1. \tag{2.2}$$

The temporal variation will be given by $e^{-i\omega t}$, where ω is the frequency of the mode. Using this, the perturbation ρ' in a scalar quantity like the density ρ can be written as

$$\rho'(r,\theta,\phi,t) = \sqrt{4\pi}\Re\left[\rho'(r)Y_l^m(\theta,\phi)e^{-i\omega t}\right], \tag{2.3}$$

where $\Re[\ ]$ denotes the real part of a complex number. Due to the assumed spherical symmetry, the frequency ω will be independent of m and depend on the radial part of the eigenfunction of the mode, which is again described by the degree l and the radial order n, which is the number of nodes in the radial eigenfunctions.

Similarly, the displacement $\delta\mathbf{r}$ can be written as

$$\delta\mathbf{r}(r,\theta,\phi,t) = \sqrt{4\pi}\Re\left[e^{-i\omega t}\left(\xi_{r,nl}(r)Y_l^m\mathbf{a}_r + \xi_{h,nl}(r)\left(\frac{\partial Y_l^m}{\partial\theta}\mathbf{a}_\theta + \frac{1}{\sin\theta}\frac{\partial Y_l^m}{\partial\phi}\mathbf{a}_\phi\right)\right)\right], \tag{2.4}$$

where ξ_r and ξ_h are the radial and horizontal displacement eigenfunctions, and $\mathbf{a}_r$, $\mathbf{a}_\theta$ and $\mathbf{a}_\phi$ are unit vectors in the r, θ, and ϕ directions. Often η is defined as $L\xi_h$ (with $L = \sqrt{l(l+1)}$) and the subscript $_r$ is dropped on the radial displacement.

The displacements $\xi(r)$ and $\eta(r)$ may be found from the equilibrium structure of the Sun, as described in Christensen-Dalsgaard and Berthomieu (1991).

It turns out that there are three basic types of solution to the oscillations equations, namely the so-called p-, g-, and f-modes. The p-modes are essentially sound waves, that is, the restoring force is provided by pressure (giving the name p-modes). These modes are the most easily observed on the Sun. The different p-modes with a given l are classified by the number n of nodes in the eigenfunctions as a function of radius (there are some problems with this counting scheme at low l). As described later, the p-modes can also be described as the interference between propagating sound waves, using so-called ray theory.

The g-modes are internal gravity modes, for which the restoring force is provided by gravity. The different solutions are again characterized by the number of nodes in the eigenfunction, but to distinguish them from the p-modes, they are generally given negative n. There are no convincing observations of g-modes on the Sun.

The f-modes are surface gravity modes (like waves on a pond) and are generally given $n = 0$. The f-modes are fairly easily observed at high l, and although the restoring force is gravity, their frequencies behave more like those of the p-modes than like those of the g-modes, as illustrated in figure 2.2.

Examples of the radial displacement functions ξ for selected p-modes have been shown in figure 2.1, and frequencies as a function of l and n for p- and f-modes are shown in figure 2.2. Both figures used results from Christensen-Dalsgaard (private communications).

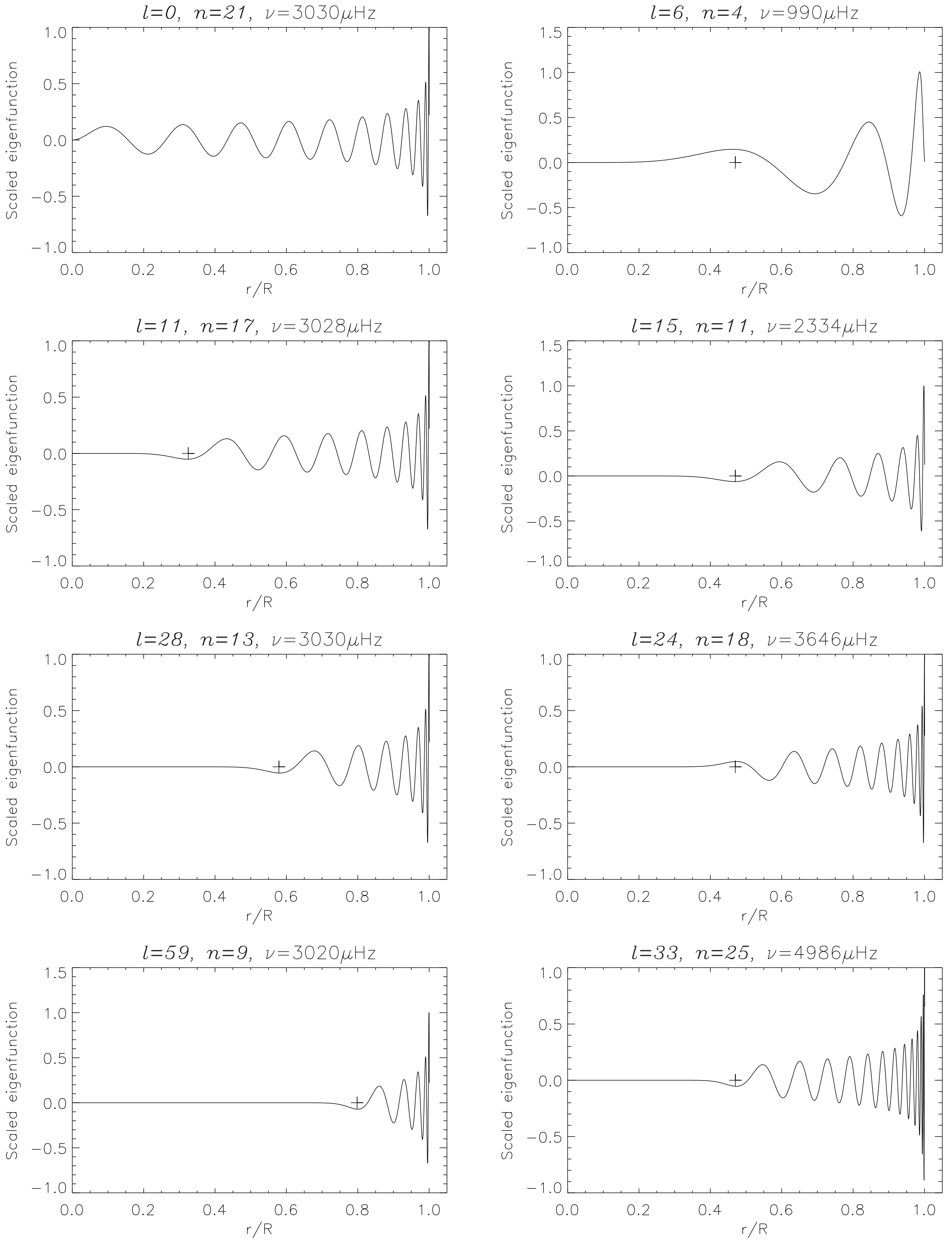

Figure 2.1: Eigenfunctions for selected (n, l). n, l, and ν have been indicated on the plots. The quantity plotted is $r\sqrt{\rho}\xi_r(r)$. The left-hand column shows a series of modes with approximately the same frequency, the right-hand column a series of modes with roughly the same ν/L. The turning points r_t have been indicated by crosses.

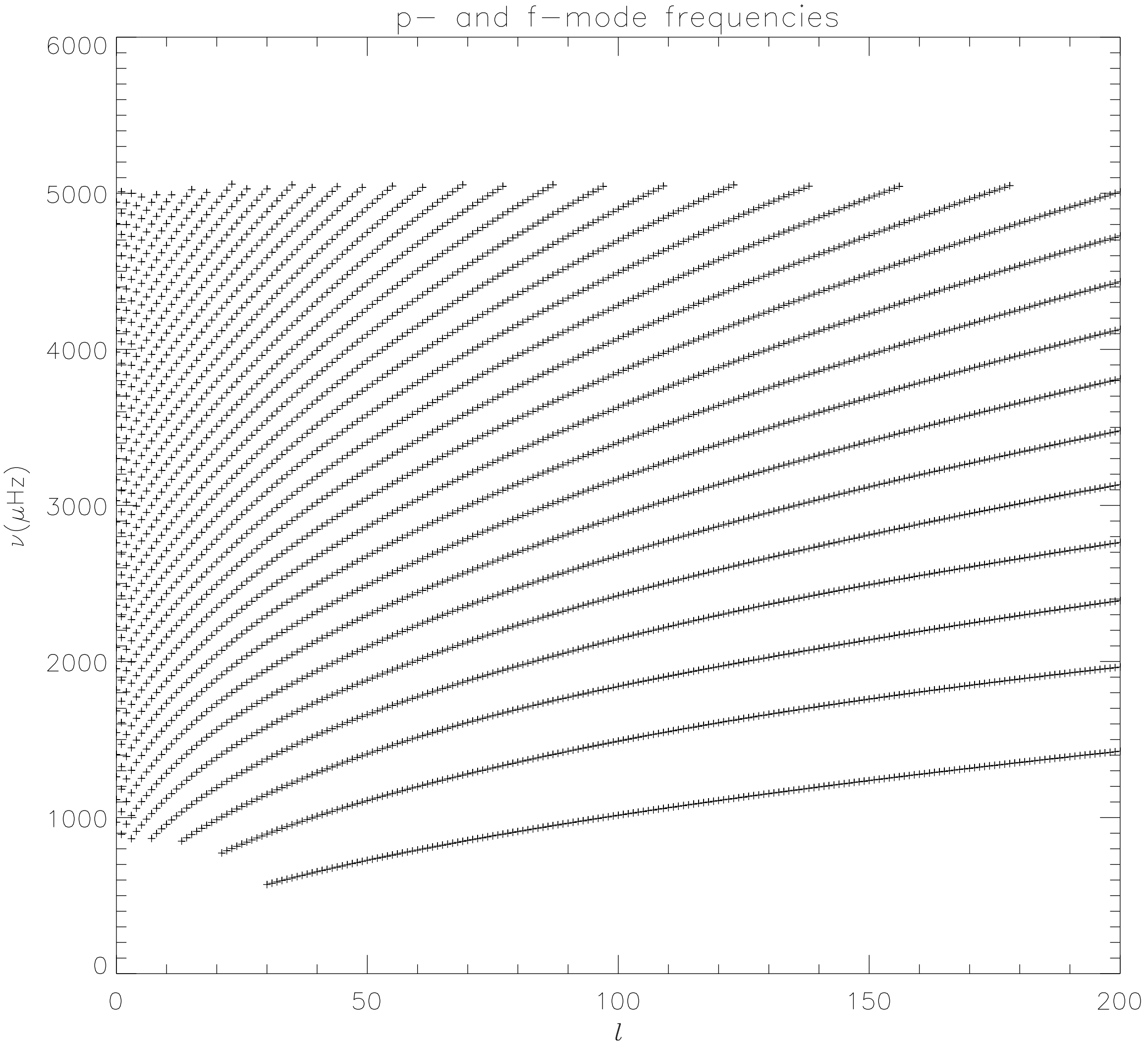

Figure 2.2: Frequencies for p- and f-modes. Only modes with $0 \le l \le 200$ have been shown. The lowest ridge is the f-mode ridge.

As can be seen from figure 2.1, the eigenfunctions for the p-modes behave in a sinusoidal way between the surface and the so-called turning point radius r_t, inside of which they are evanescent. The cause for both these behaviors is best seen if one considers that the p-modes are standing sound waves, in which case the sinusoidal pattern is simply the interference pattern of the ingoing and outgoing waves. Notice how the modes with similar frequencies in the left-hand column of figure 2.1 have similar behavior outside of the turning point.

To see why the sound waves turn at some depth r_t, consider a mode with frequency ω and degree l. As l is basically the total number of waves around the Sun (the number along the equator, given by m and the number along a meridian $l - m$, for a total of l), it follows that the horizontal wavenumber k_h in the direction of the wave propagation of each component wave is given by

$$k_h = \frac{L}{r}, \tag{2.5}$$

where L, for various reasons, turns out be the proper thing to use instead of l. The dispersion relation for a sound wave is given by

$$k^2 = k_r^2 + k_h^2 = \frac{\omega^2}{c(r)^2}, \tag{2.6}$$

where $c(r)$ is the local sound speed and thus

$$k_r^2 = \frac{\omega^2}{c(r)^2} - \frac{L^2}{r^2}. \tag{2.7}$$

If the sound wave is to be able to propagate, the horizontal wavenumber k_r^2 must be ≥ 0, and thus, r must be larger than r_t given by

$$\frac{\omega^2}{c(r_t)^2} = \frac{L^2}{r_t^2}. \tag{2.8}$$

Notice how modes with similar ν/L shown in the right-hand column of figure 2.1 penetrate to similar depths.

It actually turns out that a large number of the properties of solar oscillations can be derived using this so-called ray theory (Gough 1984, 1986). Various asymptotic approximations also exist, and while they are less accurate than the full theory, they give considerable physical insight.

Looking at figure 2.2, it is obvious that the frequencies behave in a very regular way as a function of n and l for both high and low l. For the low degree modes

$$\nu_{nl} = (n + \frac{l+0.5}{2} + \alpha)\Delta\nu, \tag{2.9}$$

where α is essentially the sum of the phase changes at the upper and lower turning points, and

$$\Delta\nu = \left(2\int_0^R \frac{dr}{c}\right)^{-1} \approx 135\mu Hz \tag{2.10}$$

is the inverse of the travel time of a wave from the center of the Sun to the surface and back. From this equation it follows that $\nu_{nl} = \nu_{n-1l+2}$, which is easily observed to be approximately satisfied. The deviation

$$\delta\nu_{nl} = \nu_{nl} - \nu_{n-1l+2} \tag{2.11}$$

from this relation turns out to be determined by the conditions in the solar core. These two frequency 'splittings' are likely to be one of the first things measured for other solar-like stars than the Sun. Actually, a so-called JCD diagram (from J. Christensen-Dalsgaard 1988), which is like an asteroseismological H-R diagram, when constructed, gives information about the mass and central hydrogen abundance of a star.

For the high-degree modes, it may be shown that

$$\omega_{nl}^2 \approx \frac{2}{\mu_p}\frac{g}{R}(n + \alpha')L \tag{2.12}$$

where $\mu_p = 1/(\Gamma_1 - 1)$ and α' is roughly a constant. From this it follows that a rough approximation to the frequencies is given by

$$\nu_{nl} = \left(\frac{nl}{60}\right)^{1/2} mHz. \tag{2.13}$$

For the f-modes a simple and very good approximation to the frequencies is given by

$$\nu_{0l} = 0.1 l^{0.5} mHz. \tag{2.14}$$

2.3 Effects of Rotation and Other Asphericities

In the previous section it was assumed that the solar structure was spherically symmetric. However, it is well known and easily observed that the Sun is far from spherically symmetric, even when only considering time-averaged quantities (and neglecting eg., convective motions and sunspots), in particular the Sun is slowly rotating.

Fortunately, the solar rotation is very slow; the rotational period is very long compared to the dynamical timescale. This convenient fact allows one to treat the rotation as a perturbation to the structure, and use standard perturbation theory to determine the perturbation to eg. the frequencies.

The dominant effect of the rotation is the advection of the oscillations. If the solar rotation rate $\Omega(r,\theta)$ were independent of radius and latitude, $\Omega(r,\theta) = \Omega_0$, and the Coriolis effect (and various other high-order effects like the centrifugal force) is neglected, the oscillation frequencies would be unaffected by the rotation if viewed from a reference frame rotating with the Sun. As the observer rotates with an angular frequency of Ω_0 in this reference frame, a mode with a frequency of ω, which in the solar reference frame looks like

$$V_r(\theta,\phi) = P_l^m(\cos\theta) e^{im\phi} e^{-i\omega t} \tag{2.15}$$

in eg. radial velocity, will look like

$$V_r(\theta,\phi') = P_l^m(\cos\theta) e^{im\phi'} e^{-i\omega t} = P_l^m(\cos\theta) e^{im(\phi-\Omega_0 t)} e^{-i\omega t} = P_l^m(\cos\theta) e^{im\phi} e^{-i(\omega+m\Omega_0)t} \tag{2.16}$$

in the observer's frame, where ϕ' is the longitude measured in a frame fixed with respect to the observer, and will thus appear to have its frequency shifted by an amount $\Delta\omega_{nlm} = m\Omega_0$.

If the rotation is not uniform, but again neglecting the Coriolis effect, the frequency shift will be m times an average of the rotation rate weighted by the energy density of the mode at each position in the Sun (or equivalently the travel time of the interferring waves across the region):

$$\begin{aligned}\Delta\omega_{nlm} &= m\frac{\int_0^R\int_0^\pi \left(\xi_{nl}(r)^2 + \eta_{nl}(r)^2\right) P_l^m(\cos\theta)^2 \Omega(r,\theta)\sin\theta\rho(r)r^2 d\theta dr}{\int_0^R\int_0^\pi \left(\xi_{nl}(r)^2 + \eta_{nl}(r)^2\right) P_l^m(\cos\theta)^2 \sin\theta\rho(r)r^2 d\theta dr} \\ &= m\frac{\int_0^R\int_0^\pi \left(\xi_{nl}(r)^2 + \eta_{nl}(r)^2\right) P_l^m(\cos\theta)^2 \Omega(r,\theta)\sin\theta\rho(r)r^2 d\theta dr}{\int_0^R \left(\xi_{nl}(r)^2 + \eta_{nl}(r)^2\right)\rho(r)r^2 dr},\end{aligned} \tag{2.17}$$

which actually turns out to be a very good approximation for high l modes, if the rotation rate is not varying too rapidly with latitude.

If a proper perturbation analysis is performed, it turns out that the frequency perturbation is given by

$$\Delta\omega_{nlm} \equiv \omega_{nlm} - \omega_{nl} \ = \ \int_0^R \int_0^\pi K_{nlm}(r,\theta)\,\Omega(r,\theta)\,r\,dr\,d\theta \ , \tag{2.18}$$

where the kernels K_{nlm} are given by

$$\begin{aligned} K_{nlm} = & \frac{m}{I_{nl}} \left(\xi_{nl}(r) \left(\xi_{nl}(r) - \frac{2}{L}\eta_{nl}(r) \right) P_l^m(x)^2 \right. \\ & \left. + \frac{\eta_{nl}(r)^2}{L^2} \left(\left(\frac{dP_l^m}{dx} \right)^2 (1-x^2) - 2P_l^m \frac{dP_l^m}{dx} x + \frac{m^2}{1-x^2} P_l^m(x)^2 \right) \right) \rho(r) r \sin\theta, \end{aligned} \tag{2.19}$$

where

$$I_{nl} = \int_0^R [\xi_{nl}(r)^2 + \eta_{nl}(r)^2] \rho(r) r^2 dr, \tag{2.20}$$

as shown in eg., Hansen, Cox, and van Horn (1977).

A 'toy' example often used is that of latitude independent rotation. In this case

$$\Delta\omega_{nlm} = m \int_0^R K_{nl}(r)\Omega(r)dr \tag{2.21}$$

with

$$K_{nl} = \frac{1}{I_{nl}} \left(\xi_{nl}^2 + \eta_{nl}^2 - \frac{2}{L}\xi_{nl}\eta_{nl} - \frac{1}{L^2}\eta_{nl}^2 \right) \rho r^2. \tag{2.22}$$

Examples of these one-dimensional mode kernels are shown in the chapter on inversions.

Of course, the eigenfunctions themselves are also perturbed by the rotation. This has been discussed in Woodard (1989) and Ritzwoller and Lavely (1992), and is an effect which needs to be taken into account for high ls when observing the modes.

Other asphericities such as sound speed variations with latitude also affect the oscillation frequencies. Again it may be shown that the perturbation in frequency is a weighted average of the perturbation as a function of radius and latitude similar to eq. (2.18) and (2.19), except for the lack of the factor m in front of the integral, and with proper normalization factors.

Generally however, the observations have not been in terms of individual mode frequencies, but rather as so-called a-coefficients, as described in eg., Schou, Christensen-Dalsgaard, and Thompson (1993, cf. App. 3). When using these a-coefficients, the mode frequencies are expanded in polynomials

$$\omega_{nlm} = \omega_{nl} + 2\pi \sum_{j=1}^{j_{max}} a_j(n,l)\,\mathcal{P}_j^{(l)}(m) \ , \tag{2.23}$$

where $\mathcal{P}_j^{(l)}$ is a polynomial of degree j. These polynomials have traditionally been Legendre polynomials $\mathcal{P}_j^{(m)} = lP_j(m/l)$ or $\mathcal{P}_j^{(m)} = LP_j(m/L)$, but they may also be chosen as in Ritzwoller and Lavely (1991). For more details on these polynomials, see section 4.2, and Schou, Christensen-Dalsgaard, and Thompson (1993, cf. App. 3).

2.4 Mode Excitation and Damping

In the previous discussion it was assumed that the modes were adiabatic and that they thus have a time-independent amplitude. From observations it is clear that this is not the case; the mode amplitudes do vary with time. It appears that the modes are exponentially damped and stochastically excited; while the details of the excitation and damping are beyond the scope of this thesis, I will give some details of some of the observational effects. A review of the current theories of mode excitation and damping by Cox et al. (1991) can again be found in 'Solar interior and atmosphere'.

Basically, the modes are believed to be excited by the convective motions close to the solar surface and the excitation is therefore stochastic. There have, however, been suggestions that some modes are intrinsically unstable.

The damping is believed to be due to at least three mechanisms: radiative damping, damping by interaction with the convection, and coupling to other modes. Given that the modes will decay exponentially, it can easily be shown that the mode profile in a power spectrum is to a good approximation given by a Lorenzian

$$P(\nu) = \frac{P_{tot}/w}{1 + \left(\frac{\nu - \nu_0}{w}\right)^2}, \tag{2.24}$$

where P_{tot} is a measure of the total power in the mode, ν_0 is the frequency of the undamped mode and w is the Half Width at Half Maximum (HWHM) of the profile.

2.5 Observations

A few of the observational aspects of helioseismology were mentioned in the historical section at the beginning of this chapter, and as already mentioned, a review can be found in Hill, Deubner, and Isaak (1991).

Basically, different types of observations can be classified by their spatial resolution and whether or not they observe in intensity or Doppler velocity. The different observing techniques each have their advantages and drawbacks.

The nonresolved observations are clearly limited to observing the lowest few ls, as the integration over the solar disk will average out the high ls. Also the unresolved observations are very susceptible to noise from atmospheric transparency variations. On the other hand, the instruments can be made extremely stable.

The resolved observations obviously have the advantage that they are able to separate different ls and ms. On the other hand, it has proved difficult to determine the absolute velocities (for the velocity observations) as a function of time and position on the solar disk, leading to problems with the low l modes. The velocity observations are at a disadvantage compared to the intensity observations in that the surface velocities are predominantly vertical and that the sensitivity therefore decreases strongly towards the solar limb, leading to problems with separating different modes, as described in Schou and Brown (1993, cf. App. 4).